TECHNICAL UNIVERSITY OF CLUJ-NAPOCA

ACTA TECHNICA NAPOCENSIS

Series: Applied Mathematics, Mechanics, and Engineering
Vol. 69, Issue Special III, July, 2026

MATHEMATICAL MODEL APPLIED TO PILOT'S PHYSIOLOGICAL MEASUREMENT

Victoria RUSU, Gavrilă CALEFARIU

Abstract: *The aerospace industry continues to expand; nevertheless, statistical reports indicate that the number of aviation accidents increased in 2024 over the past decade. Among safety-enhancement strategies advocated by ICAO is the improvement of working conditions for aviation personnel. A representative initiative is the Future Sky Safety project, which advances a contemporary ergonomics paradigm through the Human Performance Envelope concept. Previous work introduced a revised definition of this concept, identified current limitations, proposed a mathematical model for examining nine ergonomic factors, and conducted physiological measurements on a pilot using a flight simulator. The aim of the present study is to compare the outcomes of the mathematical model obtained using literature-based parameter values with those derived from the simulator-based experimental data.*
Keywords: *ergonomic, human factors, Human Performance Envelope, pilots, mathematical-model, flight simulator, physiological measurements.*

1. INTRODUCTION

The aeronautical industry is evolving continuously, resulting in an increasingly complex and more tightly regulated operational system. Based on the analysis of aviation statistical data provided by the leading organizations (EUROSTAT [1], ICAO [2], EASA [3], AIAS-Romania [4]), it can be observed that in 2024, the number of aviation incidents increases relative to the 2019–2023 average, both for commercial air transport and for general aviation (non-commercial operations) [1]-[4]. Furthermore, the most frequent accident occurrence categories are: *SCF-NP* (system/component failure or malfunction (non-powerplant)), *SCF-PP* (powerplant failure or malfunction), *ARC* (abnormal runway contact) and *LOC-I* (loss of control – inflight) [1]-[4]. So, most incidents and accidents are caused by either human error or technical faults.

Therefore, it is crucial that all parties involved in the aviation industry implement suitable regulations to improve air traffic safety, both by streamlining aircraft manufacturing and maintenance procedures and by successfully attending to the requirements of operational staff (air traffic controllers and pilots).

For instance, ICAO designs and advances programs and initiatives such as Global Runway Safety Action Plan (GRSAP) and the Global Navigation Satellite System (GNSS), as the advancement of technology has led to the evolution of air surveillance systems. [5] Moreover, ICAO promotes civil–military collaboration in aviation and encourages technological innovation in weather forecasting, while also emphasizing mental well-being and the effective application of individualized risk management. [2] Examples of projects that aim to reduce the incidence of aircraft accidents and enhance safety through a human-factors approach, include: European Plan for Aviation Safety (EPAS), Future Sky Safety (founded by EREA and funded by the European Union's Horizon Program 2020), STRESS, ACROSS and others.

The "Future Sky Safety" project adopts a new paradigm in ergonomics, referred to as the Human Performance Envelope (HPE) [6],

which was firstly mentioned by Tamsyn Edwards in her PhD Thesis. [7] Instead of concentrating on a single factor (at most two) investigated in isolation—such as fatigue, stress, or situational awareness—as was typical in previous studies in the subject, this approach involves taking into account a variety of human factors in the investigation of aviation accidents. In such way, EUROCONTROL experts identified nine ergonomic factors (workload, stress, fatigue, attention, vigilance, situation awareness, teamwork, communication and trust) as both important predictors of the activities carried out by air traffic controllers and issues that could negatively impact their performance. [7]

The previously published paper [8] contains the suggested definition of the Human Performance Envelope as well as the defined concept limits in pilot's case.

2. METHODS AND MATERIALS

2.1 Methods

In the previous research [9] was tailored the Stanciulescu's mathematical-heuristic hybrid macroecomic model [10] to the HPE theory, establishing a quantitative framework for examining the dynamics of human performance.

Because six ergonomic factors—mental workload, stress, fatigue, situational awareness, attention, and vigilance—can be evaluated using physiological indicators (such as heart rate variability, respiration rate, heart rate, alpha/beta/theta brain activity, pupil diameter and blink rate) recorded with devices like eye tracking, ECG or EEG, the mathematical part of the model is well suited to HPE research. While, its heuristic component, is better suitable for psychosocial ergonomic elements (teamwork, communication and trust), which can be investigated using questionnaires, observations, interviews, or incident report analyses. [9]

As a result, the variables for the mathematical component of the variational equations were specified as follows: physiological parameters were defined as the input variables, while the six ergonomic factors were designated as the output variables (Table 1). [9]

A broad range of physiological indicators has been examined in the literature; however, the Future Sky Safety initiative consolidated the most relevant measures into a structured set of Cards [6]. These Cards served as the basis for selecting the input variables and defining their corresponding indicators. A collection of physiological variables was chosen for each ergonomic aspect based on evidence of their quantifiable impact to that factor.

For instance, with the fatigue arousal, the eye blink duration (EBD), delta band power (Pδ), theta band power (Pθ), alpha band power (Pα) and heart rate variability (HRV) increase, while pupil diameter (PD), saccadic eye rate (SR), beta band power (Pβ), heart rate (HR), muscle tension (MuscTen), respiratory rate (RR) and electrodermal activity decrease (EDA).

Table 1 [9]

Variables for mathematical model

Input variables		**Input variables**	
$HbO_2(t)$	Oxygenated Hemoglobin	*MW*	Mental Workload
HR(t)	Heart rate	*S*	Stress
HRV(t)	Heart rate variability	*F*	Fatigue
SBP(t)	Systolic blood pressure	*SA*	Situation Awareness
RR(t)	Respiratory rate	*A*	Attention
EBR(t)	Eye blink rate	*V*	Vigilance
EBD(t)	Eye blink duration		
PD(t)	Pupil diameter		
Pα(t)	Alpha band power		
Pβ(t)	Beta band power		
Pθ(t)	Theta band power		
Pδ(t)	Delta band power		
MuscTen(t)	Muscle tension		
EDA(t)	Electrodermal activity		
AD(t)	Adrenaline		
NAD(t)	Noradrenaline		
SR(t)	Saccadic rate		
MA(t)	Mental activity		
rCBFv(t)	Right cerebral blood flow velocity		

In such way, the model's mathematical component is expressed through six variational equations (1-6), plus conditions (7) and (8) which represent the effects of complicated operating circumstances in order to facilitate a more thorough assessment of human

performance. [9] In the literature, controlled platforms like flight simulators and workplace simulations are often used to simulate different complex circumstances, such as multitasking demands, technical issues, turbulence or unfavorable weather [11] – [13]. Increases in mental workload ($MW_0<MW(t)$), stress ($S_0<S(t)$), and tiredness ($F_0<F(t)$) are among the measurable physiological and cognitive changes brought about by these treatments. In contrast, situation awareness ($SA_0>SA(t)$), attention ($A_0>A(t)$), and vigilance ($V_0>V(t)$) often deteriorate over time. This approach improves the fidelity of models intended to forecast and assess performance in difficult operational environments by making it easier to mathematically describe time-varying human state dynamics under stress.

$$\frac{d}{dt}MW(t) = \alpha_1 HR(t) + \beta_1 SBP(t) + \gamma_1 RR(t) + \delta_1 PD(t) + \omega_1 P\beta(t) + \varphi_1 P\theta(t) + \eta_1 MuscTen(t) + \theta_1 EDA(t) - \kappa_1 HRV(t) - \lambda_1 EBR(t) - \mu_1 EBD(t) - \tau_1 P\alpha(t) \quad (1)$$

$$\frac{d}{dt}S(t) = \gamma_2 RR(t) + \alpha_2 HR(t) + \beta_2 SBP(t) + \eta_2 MuscTen(t) + \lambda_2 EBR(t) + \theta_2 EDA(t) + \xi_2 AD(t) + \rho_2 NAD(t) - \kappa_2 HRV(t) \quad (2)$$

$$\frac{d}{dt}F(t) = \mu_3 EBD(t) + \sigma_3 P\delta(t) + \varphi_3 P\beta(t) + \tau_3 P\alpha(t) + \kappa_3 HRV(t) - \delta_3 PD(t) - \chi_3 SR(t) - \omega_3 P\beta(t) - \alpha_3 HR(t) - \eta_3 MT(t) - \gamma_3 RR(t) - \theta_3 EDA(t) \quad (3)$$

$$\frac{d}{dt}SA(t) = \upsilon_4 MA(t) + \alpha_4 HR(t) - \kappa_4 HRV(t) - \lambda_4 EBR(t) - \mu_4 EBD(t) \quad (4)$$

$$\frac{d}{dt}A(t) = \alpha_5 HR(t) - \kappa_5 HRV(t) - \lambda_5 EBR(t) - \mu_5 EBD(t) - \tau_5 P\alpha(t) - \rho_5 rCBFv(t) \quad (5)$$

$$\frac{d}{dt}V(t) = \alpha_6 HR(t) - \kappa_6 HRV(t) - \lambda_6 EBR(t) - \mu_6 EBD(t) - \tau_6 P\alpha(t) - \rho_6 rCBFv(t) \quad (6)$$

$$MW_0 < MW(t), S_0 < S(t), F_0 < F(t) \quad (7)$$

$$SA_0 > SA(t),\ A_0 > A(t), V_0 > V(t) \quad (8)$$

2.2 Materials

Using the Beechcraft King Air C90GTx Full Flight Simulator (FFS), were conducted experimental trials. Through RSi's advanced XT6 visual system, developed specifically for business and turboprop aircraft applications, this simulator provides a highly immersive and realistic training environment. In addition, in order to enhance the representation of flight dynamics, is using the VanHalteren motion platform. [14] In such way, the Beechcraft King Air C90GTx Full Flight Simulator offers a close approximation of real-world flight conditions, being equipped with a detailed cockpit environment, highly responsive control loading and configured with high-fidelity aerodynamic models. [15]

The participant at the experiment was a pilot who had previously used the Beechcraft King Air C90GTx Full Flight Simulator (FFS) and had about 330 flight hours. Before the start of the test, a written informed permission was obtained in compliance with applicable ethical principles. Plus, the subject answered a screening questionnaire about overall health, amount of sleep hours, and other variables that might impact the psychological state. [16]

After the flight session, the pilot was asked to complete the NASA-TLX questionnaire, that creates a sensitive and accurate estimate of workload by integrating data on the size and contributing sources of six workload-related parameters. [17]

The simulated flight departed from and returned to Salzburg Airport (LOWS) using a closed-pattern flying profile. A low-level wind layer with a constant easterly component (90°) at 15 knots was one of the environmental conditions. The autopilot was turned off, necessitating constant human control. The Instrument Landing System (ILS) was used during landings. The simulation was carried out using only onboard instrumentation and no external visual references, in accordance with instrument flying regulations (IFR). [16]



Fig. 1. The experimental setup

During the experiment, pilot was wearing special equipment for physiological

measurements, (fig.1). Tobii Pro Glasses 2 eye-tracking technology was one of it, used to record eye movements and gaze behavior, allowing for the precise assessment of visual attention allocation and accompanying cognitive workload during flight-related tasks.

To offer accurate measures of fixation patterns and gaze direction, the eye-tracker is equipped with a head-mounted unit which has binocular eye-tracking sensors, infrared illumination and a high-definition scene camera. Through synchronized eye-movement data and video recordings, the system facilitates both post hoc analysis and real-time observation, allowing for the objective evaluation of visual attention under ecologically realistic conditions. [18]

Another equipment used for registering physiological signals, was BIOPAC MP160, a high-precision modular platform for physiological data collection and analysis intended for advanced life-science research. Its main unit supports: an aggregate sampling rate of up to 400 kHz, Ethernet-based connection, up to 16 analog input channels, and 16-bit analog-to-digital conversion resolution. [19]

The ECG100C/D amplifier for cardiac electrophysiology, the EEG100C/D amplifier for cerebral activity monitoring, and respiratory transducers such as the RSP100C/D for respiratory dynamics assessment were among the specialized acquisition modules used in this investigation. The AcqKnowledge software, which offers automated analysis routines for electrocardiography (ECG), heart rate variability (HRV), electroencephalography (EEG), respiration, and related physiological measures, processed the recordings that resulted from the simultaneous integration of these modules with the MP160 system.

A thorough examination of the relationships between pilot physiology, visual attention, and task performance was made possible by the incorporation of these measurement tools into the simulated flight environment. This methodology permitted the synchronized gathering of multimodal data under conditions that were both realistic and regulated, so ensuring participant safety and experimental rigor.

2.3 Physiological data analysis

All signals were methodically processed and examined following the collection of physiological and eye-tracking data utilizing the BIOPAC system and Tobii Pro Glasses 2. AcqKnowledge (BIOPAC), which facilitates signal visualization, processing, and quantitative analysis, was used to analyze important metrics, such as heart rate, heart rate variability, breathing, and EEG activity. Initially stored as voltage time series (μV), ECG recordings were converted to beats per minute (BPM) using AcqKnowledge's Find Rate function (fig.2), which identifies subsequent cardiac cycles and outputs a dedicated heart-rate waveform in BPM, in order to conform to standard reporting conventions.

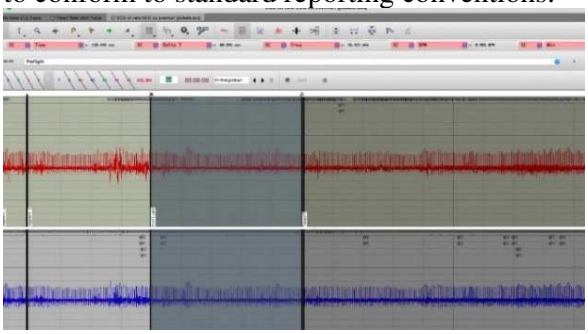


Fig. 2. ECG - Heart rate in AcqKnowledge

The Find Rate function in AcqKnowledge calculates rate-related outputs by identifying cyclic characteristics (like peaks) in physiological waveforms. Depending on parameters, it might rely on simple thresholding or improved peak-detection features such as noise rejection and temporal windowing. The tool can return metrics including frequency (Hz), peak amplitudes (min/max), peak-to-peak intervals, signal area, and mean values in addition to beats per minute (BPM).

Respiration data were treated in the same way, while heart rate variability (HRV) was measured with the Multi-Epoch HRV Statistical function from the Analysis menu. After processing the ECG data, was produced an Excel file with parameters including left edge, right edge, RMSSD, SDSD, and pNN50. Since RMSSD metric is the most widely used and widely published indication of HRV in the scientific literature, its values were used for the purposes of this investigation. [16]

The EEG band signals (alpha, beta, delta, theta, and gamma) were not further processed; instead, the recordings were exported as CSV files and subsequently analyzed in Excel. Prior to export, focus areas corresponding to each flight phase (preflight, takeoff, cruise, and landing) were defined in AcqKnowledge. This enabled phase-specific analyses, particularly the computation of mean values for key physiological measures (HR, RR, Pα, Pβ, and Pθ) across the different flight segments.

Tobii Pro Lab (fig.3) was used to process the eye-tracking recordings from the Tobii Pro Glasses 2. Key flight events (such as takeoff, cruise, and landing commencement) were identified and annotated by importing experiment that was saved on the device SD card. The Metrics and Data Export features were then used to export fixation metrics, pupil diameter, and gaze location to Excel.



Fig. 3. Heatmap in Tobii Pro Lab

Pupil diameter served as the main eye-tracking variable in this investigation. Marcus Nyström's approach was used to derive blink duration and frequency [20]. The pupil-diameter-based method, which uses variations in pupil size to calculate blink-related metrics, was implemented in Python since Tobii Pro Glasses 2 does not include any eye-openness measurements. Additionally, the final dataset was exported to Excel for further analysis after being divided into flight phases in Python.

3. RESULTS

In prior work [9], the estimation of the unknown model coefficients in equation (1) was approached by recasting the governing relation into a fully determined linear system solvable via Cramer's rule. Because equation (1) contains twelve unknown parameters, an additional eleven independent instances of the same relationship were formulated, resulting in a total of twelve equations. These equations were obtained by substituting physiologically plausible input values—extracted from published studies—into the model structure, thereby generating a 12×12 system with the same number of equations as unknowns (equation (9)). In matrix form, this procedure yields a coefficient matrix assembled from the selected physiological variables and a corresponding right-hand-side vector defined by the prescribed mental workload term, enabling a closed-form solution for the parameter vector when the system is non-singular.

$$\begin{cases} \alpha_1 81 + \beta_1 211{,}5 + \gamma_1 16{,}5 + \delta_1 3{,}79 + \omega_1 0{,}72 + \varphi_1 0{,}58 + \eta_1 22 + \theta_1 10{,}14 - \kappa_1 31 - \lambda_1 7{,}9 - \mu_1 567 - \tau_1 0{,}58 = \frac{dMW}{dt} \\ \alpha_1 73 + \beta_1 110{,}8 + \gamma_1 13 + \delta_1 3{,}85 + \omega_1 0{,}92 + \varphi_1 0{,}85 + \eta_1 19 + \theta_1 2{,}7 - \kappa_1 27 - \lambda_1 4{,}5 - \mu_1 420 - \tau_1 0{,}78 = \frac{dMW}{dt} \\ \alpha_1 73{,}5 + \beta_1 112{,}3 + \gamma_1 13{,}5 + \delta_1 3{,}93 + \omega_1 0{,}93 + \varphi_1 0{,}86 + \eta_1 20 + \theta_1 2{,}97 - \kappa_1 28 - \lambda_1 5{,}0 - \mu_1 425 - \tau_1 0{,}79 = \frac{dMW}{dt} \\ \alpha_1 74 + \beta_1 114{,}2 + \gamma_1 14 + \delta_1 3{,}94 + \omega_1 0{,}94 + \varphi_1 0{,}87 + \eta_1 21 + \theta_1 3{,}94 - \kappa_1 29 - \lambda_1 5{,}2 - \mu_1 430 - \tau_1 0{,}80 = \frac{dMW}{dt} \\ \alpha_1 74{,}5 + \beta_1 120{,}8 + \gamma_1 14{,}5 + \delta_1 3{,}95 + \omega_1 0{,}95 + \varphi_1 0{,}88 + \eta_1 22 + \theta_1 4{,}98 - \kappa_1 30 - \lambda_1 5{,}5 - \mu_1 435 - \tau_1 0{,}81 = \frac{dMW}{dt} \\ \alpha_1 75 + \beta_1 121{,}7 + \gamma_1 15 + \delta_1 3{,}96 + \omega_1 0{,}96 + \varphi_1 0{,}89 + \eta_1 23 + \theta_1 7{,}64 - \kappa_1 31 - \lambda_1 6 - \mu_1 440 - \tau_1 0{,}82 = \frac{dMW}{dt} \\ \alpha_1 75{,}5 + \beta_1 123{,}7 + \gamma_1 15{,}5 + \delta_1 4{,}05 + \omega_1 0{,}97 + \varphi_1 0{,}90 + \eta_1 24 + \theta_1 7{,}81 - \kappa_1 32 - \lambda_1 6{,}5 - \mu_1 445 - \tau_1 0{,}83 = \frac{dMW}{dt} \\ \alpha_1 76 + \beta_1 131{,}2 + \gamma_1 15{,}7 + \delta_1 4{,}06 + \omega_1 0{,}98 + \varphi_1 0{,}91 + \eta_1 25 + \theta_1 11{,}92 - \kappa_1 33 - \lambda_1 6{,}7 - \mu_1 450 - \tau_1 0{,}84 = \frac{dMW}{dt} \\ \alpha_1 76{,}5 + \beta_1 139{,}2 + \gamma_1 16 + \delta_1 4{,}10 + \omega_1 0{,}99 + \varphi_1 0{,}92 + \eta_1 26 + \theta_1 12{,}90 - \kappa_1 34 - \lambda_1 7 - \mu_1 455 - \tau_1 0{,}85 = \frac{dMW}{dt} \\ \alpha_1 77 + \beta_1 157{,}5 + \gamma_1 16{,}5 + \delta_1 4{,}14 + \omega_1 1 + \varphi_1 0{,}93 + \eta_1 27 + \theta_1 13{,}77 - \kappa_1 35 - \lambda_1 7{,}5 - \mu_1 460 - \tau_1 0{,}86 = \frac{dMW}{dt} \\ \alpha_1 77{,}5 + \beta_1 162{,}9 + \gamma_1 16{,}7 + \delta_1 4{,}15 + \omega_1 1{,}01 + \varphi_1 0{,}94 + \eta_1 28 + \theta_1 22{,}63 - \kappa_1 36 - \lambda_1 8 - \mu_1 465 - \tau_1 0{,}87 = \frac{dMW}{dt} \\ \alpha_1 78 + \beta_1 163{,}9 + \gamma_1 17 + \delta_1 4{,}16 + \omega_1 1{,}02 + \varphi_1 0{,}95 + \eta_1 29 + \theta_1 35{,}7 - \kappa_1 37 - \lambda_1 8{,}5 - \mu_1 468 - \tau_1 0{,}88 = \frac{dMW}{dt} \end{cases} \quad (9)$$

The final mean was computed as the arithmetic average of values extracted from independent sources. Studies were identified via databases ScienceDirect, IEEE, Web of Science, and searching academic platform Google Scholar, and were selected if they assessed pilot or air-traffic-controller mental workload using physiological measures. Priority was given to highly cited studies with larger samples. When multiple estimates for the same variable were reported within a study, they were averaged to obtain a single representative value. [9]

In the previous study, the system could not be fully solved due to practical constraints.

Subsequently, the system was completed by supplementing the missing elements and finalizing the coefficient estimation procedure, thereby obtaining a complete parameter set. Building on that completed solution, the present study performs a comparative evaluation using two distinct input datasets: variable values extracted from the literature (representing previously reported workload - related physiological responses) and variables measured directly during the simulated-flight experiment.

This study evaluates how well the model parameters—and the workload dynamics that the model infers—remain consistent when switching from diverse, literature-derived measurements to controlled, simulator-based recordings by using the same Cramer-based framework on both datasets. In addition to highlighting potential sources of disparity, such as variations in measurement equipment, preprocessing pipelines, participant characteristics, and the experimental setting in which the physiological responses were triggered, this comparison offers an explicit test of the model's resilience.

To solve the system of equation (9), an estimate of the time derivative of mental workload, $\frac{dMW}{dt}$, was required as the right-hand-side term of the variational formulation. This derivative was obtained from the workload profile $MW(t)$ by interpreting $\frac{dMW}{dt}$ as the instantaneous rate of change of workload with respect to time. Accordingly, the derivative at selected time instants was approximated as the slope of the tangent to the $MW(t)$ curve (Fig. 4).

Because the workload trajectory was available as discrete points on the graph, the tangent slope was computed using a finite-difference approximation between two neighboring points (x_1, y_1) and (x_2, y_2) surrounding the time of interest. Thus, the derivative was estimated as

$$\frac{dMW}{dt} = \frac{(y_2 - y_1)}{(x_2 - x_1)} = tg\alpha \qquad (10)$$

where α is the angle between the tangent line and the positive time axis. The resulting $\frac{dMW}{dt}$ values were then used to populate the vector b in the linear system, equation (9), enabling the computation of the unknown coefficient vector through the chosen solution method.

Accordingly, equation (10) was applied to the workload profile to obtain a representative value for the mental workload term, resulting in $\frac{dMW}{dt} = 2{,}55$. This value was then used to define the right-hand-side of the linear identification problem.

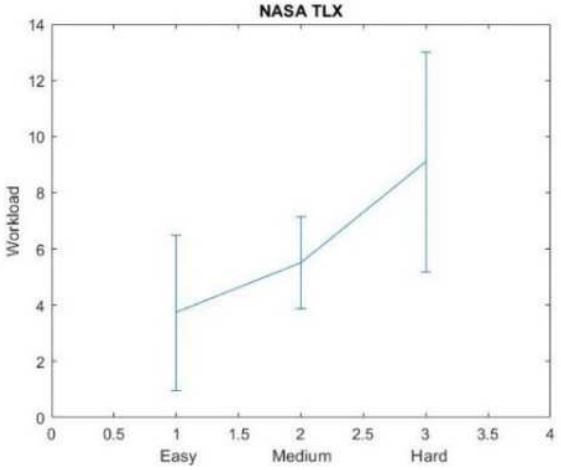


Fig. 4. NASA-TLX graph [11]

Specifically, the variational formulation in equation (9) contains twelve unknown coefficients; therefore, a corresponding set of twelve independent equations was assembled by substituting literature-derived physiological values into the model structure. The resulting system can be expressed compactly in matrix form as

$$A\,x = b \qquad (11)$$

where $A \in \mathbb{R}^{12\times12}$ is the coefficient matrix whose entries are formed from the selected physiological variables (and their prescribed signs in the model), $x \in \mathbb{R}^{12\times1}$ is the vector of unknown model coefficients, and $b \in \mathbb{R}^{12\times1}$ is the target vector associated with the workload term.

In this implementation, b was constructed as a constant vector with all entries equal to 2,55, reflecting the assumed workload value for each of the twelve equation instances. The system was then implemented in MATLAB as a 12×12 matrix problem, and equation (11) was used to compute the solution vector x (reported in equation (12)), thereby yielding the

estimated coefficients that satisfy equation (9) under the adopted literature-based inputs and workload target.

Using this framework, the mathematical model was partially validated by applying the derived coefficient set to datasets reported in the literature for mental workload (equation (1)).

Specifically, literature-derived physiological measurements served as surrogate inputs for the variational variables, while the mental workload values reported in those studies provided reference targets against which the model output could be assessed. This partial validation established an initial level of consistency between the proposed model structure and empirically observed workload-related responses.

$$x = \begin{cases} 0{,}0476 \\ 0 \\ 0 \\ 0 \\ -12{,}2704 \\ 4{,}3604 \\ -0{,}1037 \\ 0 \\ -0{,}0740 \\ 0 \\ 0 \\ -8{,}5027 \end{cases} \quad (12)$$

In order to apply the same procedure on the physiological measurements obtained during the simulated flight, the data gathered from the wearable equipment was analyzed as described in Section 2.3, and the obtained results were subsequently presented in Table 2.

It should be noted that, relative to the variables reported in the literature, a reduced set of measures (HR, RR, HRV, Pα, Pβ, Pθ, PD and EBR) was collected in the present study due to the constraints of the available wearable equipment.

Subsequently, the system of equations (13) was formulated, comprising eight variational equations. In this system, the input variables were replaced with their corresponding mean values (Table 2), the coefficients were retained unchanged, and mental workload (MW) was treated as the output variable.

Following the simulated flight, the pilot completed the NASA-TLX questionnaire by assigning 0–100 ratings to the six workload dimensions (Mental, Physical, Temporal, Performance, Effort, and Frustration) for each flight phase. The mean of these ratings was then used as the basis for constructing the workload graph. (fig.5)

Table 2

Mean values of variables by flight phase

Flightphase	HR_mean	RR_mean	Pα_mean	Pβ_mean	Pθ_mean	EBR_mean	PD_mean	RMSSD
Preflight	91,58	31,69	0,0000	0,0000	0,0000	0,18	4,63	500,45
Takeoff	93,99	9,25	0,0008	-0,0012	0,0008	0,47	4,82	552,88
Cruise1	90,25	8,39	0,0007	0,0003	-0,0024	0,33	4,69	478,10
Cruise2	87,05	7,64	0,0004	-0,0007	0,0007	0,38	4,52	528,20
Cruise3	89,58	8,83	-0,0013	-0,0011	-0,0030	0,32	4,64	481,69
Cruise4	90,04	8,77	-0,0002	-0,0002	0,0000	0,55	4,71	515,14
Cruise5	92,46	10,54	-0,0005	-0,0005	-0,0001	0,57	4,52	519,06
Landing	98,48	7,02	0,0003	0,0000	-0,0020	0,25	4,50	456,01

$$\begin{cases} \alpha_1 91{,}58 + \gamma_1 31{,}69 + \delta_1 4{,}63 + \omega_1 0{,}0048 + \varphi_1 0{,}0035 - \kappa_1 500{,}45 - \lambda_1 0{,}1821 - \tau_1 0{,}0041 = \frac{dMW}{dt} \\ \alpha_1 93{,}99 + \gamma_1 9{,}25 + \delta_1 4{,}82 - \omega_1 0{,}0012 + \varphi_1 0{,}0008 - \kappa_1 552{,}88 - \lambda_1 0{,}4709 - \tau_1 0{,}0008 = \frac{dMW}{dt} \\ \alpha_1 90{,}25 + \gamma_1 8{,}39 + \delta_1 4{,}69 + \omega_1 0{,}0003 - \varphi_1 0{,}0024 - \kappa_1 478{,}1 - \lambda_1 0{,}3303 - \tau_1 0{,}00075 = \frac{dMW}{dt} \\ \alpha_1 87{,}05 + \gamma_1 7{,}64 + \delta_1 4{,}52 - \omega_1 0{,}0007 + \varphi_1 0{,}0007 - \kappa_1 528{,}20 - \lambda_1 0{,}3847 - \tau_1 0{,}00036 = \frac{dMW}{dt} \\ \alpha_1 89{,}58 + \gamma_1 8{,}83 + \delta_1 4{,}64 - \omega_1 0{,}0011 - \varphi_1 0{,}0030 - \kappa_1 481{,}69 - \lambda_1 0{,}3200 + \tau_1 0{,}0013 = \frac{dMW}{dt} \\ \alpha_1 90{,}04 + \gamma_1 8{,}77 + \delta_1 4{,}71 - \omega_1 0{,}0002 + \varphi_1 0{,}00003 - \kappa_1 515{,}14 - \lambda_1 0{,}5515 + \tau_1 0{,}00019 = \frac{dMW}{dt} \\ \alpha_1 92{,}46 + \gamma_1 10{,}54 + \delta_1 4{,}52 - \omega_1 0{,}0005 - \varphi_1 0{,}0002 - \kappa_1 519{,}06 - \lambda_1 4{,}5241 + \tau_1 0{,}00052 = \frac{dMW}{dt} \\ \alpha_1 98{,}48 + \gamma_1 7{,}02 + \delta_1 4{,}50 + \omega_1 0{,}00002 - \varphi_1 0{,}0020 - \kappa_1 456{,}01 - \lambda_1 0{,}2542 - \tau_1 0{,}00032 = \frac{dMW}{dt} \end{cases} \quad (13)$$

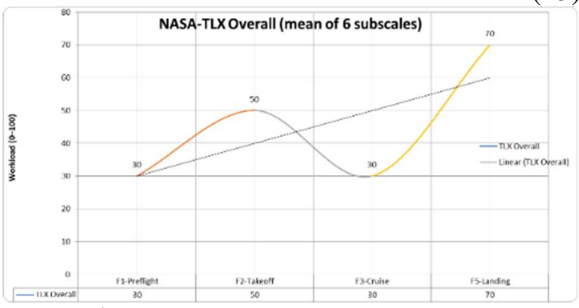


Fig. 5. NASA-TLX graph for experiment

Subsequently, the time derivative of mental workload, $\dot{MW}(t)$, was determined by applying formula (10) to the values extracted from the

workload profile (NASA-TLX) shown in Fig. 5. Specifically, the discrete points obtained from the graph were used to compute the corresponding rate of change in workload with respect to time, thereby providing an empirical estimate of $\frac{d}{dt}MW(t)$ over the analyzed interval.

Using this derived quantity as the right-hand-side term, mathematical expression (11) was then employed to compute the coefficient vector x. In this formulation, the matrix A contains the physiological input variables (arranged according to the defined variational representation), while the vector b is formed from the estimated derivative values. Solving the resulting linear system in Matlab program (fig. 6), yielded the vector x, reported in system of solutions (14), which represents the unknown model coefficients associated with each physiological predictor.

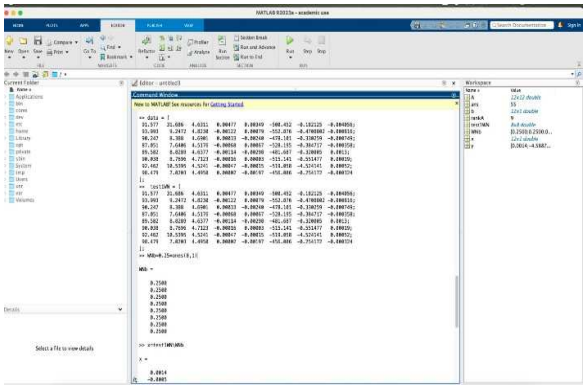


Fig. 6. Solving the system of equations in Matlab

$$x = \begin{cases} 0{,}0014 \\ -0{,}0005 \\ -0{,}0493 \\ 13{,}75600 \\ -9{,}1778 \\ -0{,}0007 \\ 0{,}0034 \\ 5{,}2868 \end{cases} \quad (14)$$

4. DISCUSSION

Significant differences in both sign and magnitude are observed when comparing the coefficients estimated from literature-derived inputs with those obtained from the simulated-flight dataset (Table 3).

In the simulator-based solution, the cardiorespiratory terms receive substantially lower weights, with the HR coefficient decreasing from 0,0476 to 0,0014 and the HRV coefficient decreasing from −0,0740 to −0,0007. Coefficients associated with respiration rate and blink rate are close to zero (RR: 0 vs. −0,0005; EBR: 0 vs. 0,0034), indicating a negligible contribution under the present estimation setup. In contrast, pupil diameter emerges as a non-trivial predictor in the experimental solution (PD: 0 vs. −0,0493), whereas it is not retained in the literature-based coefficient set.

Table 3

Comparison of model coefficients (literature vs. experimental results)

Input variables	Results from literature	Results from experiment
HR – α_1	0,0476	0,0014
RR – γ_1	0	-0,0005
PD – δ_1	0	-0,0493
Pβ – ω_1	-12,2704	13,75600
Pθ – φ_1	4,3604	-9,1778
HRV – κ_1	-0,0740	-0,0007
EBR – λ_1	0	0,0034
Pα – τ_1	-8,5027	5,2868

The largest discrepancies occur for the EEG-derived variables, which dominate the experimental coefficient magnitudes and exhibit sign reversals relative to the literature coefficients (Pβ: −12,2704 vs. 13,7560; Pθ: 4,3604 vs. −9,1778; Pα: −8,5027 vs. 5,2868). Collectively, these results suggest that, for the simulator dataset, EEG-related predictors (together with PD) primarily drive the fitted solution, whereas HR and HRV contribute only marginally.

However, without harmonized preprocessing and feature definitions, the raw coefficients are not directly transferable between datasets. Discrepancies may arise from differences in how predictors are computed (e.g., absolute vs. relative/log band power, or band-pass waveforms vs. power features), unit scaling and normalization, and inter-variable dependence—particularly among EEG band measures—leading to instability and sign changes when fitting multiple coefficients from a limited number of

independent observations. Consequently, the estimated coefficients should be interpreted as dataset-specific sensitivities rather than universal physiological weights, motivating the use of standardized predictors and more stable identification methods (regularized or constrained regression) for robust cross-study comparisons.

Additional contributors to the observed differences may include variations in measurement equipment and sensor configurations, the limited number of experimental participants, and potential subjectivity in NASA-TLX workload ratings.

5. CONCLUSION

Although the aerospace sector continues to evolve, safety analyses indicate that human factors remain a major contributor to aviation accidents. Accordingly, improving the assessment and support of aviation personnel is essential for reducing operational error within the aeronautical socio-technical system. In this context, the Future Sky Safety project operationalized the Human Performance Envelope (HPE) concept for pilot applications, providing a structured framework comprising nine ergonomic factors defined by EUROCONTROL experts.

Building on prior work, this study applied a hybrid mathematical–heuristic modeling approach in which the mathematical component targets physiologically grounded factors (mental workload, stress, fatigue, situation awareness, attention, and vigilance), while the heuristic component addresses psychosocial factors (communication, trust, and teamwork). The present work evaluated the consistency of the mathematical component by comparing Cramer-based model coefficients estimated from literature-derived values with coefficients obtained from physiological measurements collected during a simulated-flight experiment.

The comparison revealed substantial discrepancies in both magnitude and sign between the two coefficient sets, indicating that the raw parameters are not directly transferable across datasets. These differences are plausibly driven by non-harmonized preprocessing, inconsistent feature definitions (e.g., band-pass waveforms versus true band-power measures; absolute versus relative/log power), scaling and normalization effects, inter-variable dependence (particularly among EEG predictors), and identifiability limitations when estimating multiple coefficients from a limited number of independent observations.

Consequently, the estimated coefficients should be interpreted as dataset-specific sensitivities rather than universal physiological weights, motivating future work focused on harmonized preprocessing pipelines, standardized predictors, and more robust identification strategies (e.g., regularized or constrained regression), alongside larger participant samples and improved workload ground truth to support reliable cross-study comparisons.

6. REFERENCES

[1] EUROSTAT, Raport *Air safety statistics in EU. Statistics explained.*, september 2025, https://ec.europa.eu/eurostat/statistics-explained/index.php?title=Air_safety_statistics_in_the_EU

[2] ICAO, Safety Report, *State of global aviation safety*, 2025 Edition, https://www.icao.int/safety-reports

[3] EASA, Raport, *Annual safety review 2025*, DOI 10.2822/7481215

[4] AIAS, *Safety annual report 2024*, 2025, https://aias.gov.ro/studii-si-analize/raport-anual-privind-siguranta-2024/

[5] Găină, L., Meclea, M. A., Boșcoianu, M., *Research on the maintenance of air surveillance systems management in the context of technological development industry 4.0.* Scientific Research & Education in the Air Force-AFASES, 2021.

[6] Silvagni, S., Napoletano, L., Graziani, I., Le Blaye, P., Rognin, L., *Concept for Human Performance Envelope*, Future Sky Safety project, initiated by European Research Establishments in Aeronautics (EREA), document D6.1, 2015.

[7] Tamsyn, E., PhD Thesis: *Human performance in air traffic control*, University from Nottingham, 2013.

[8] Rusu, V., Calefariu, G., *Definition and literature review on Human Performance Envelope Concept in aerospace activity*,

Recent J., 63:041-9, 2021, DOI:10.31926/RECENT.2021.63.041.
[9] Rusu, V., Calefariu, G., *Mathematical-heuristic modelling for human performance envelope*, Human Systems Management, vol. 42, no. 2, pp. 233-246., 2023.
[10] Stanciulescu, F., *Modelarea sistemelor de mare complexitate*, Editura Tehnica, pg. 77-92, 2003, Bucharest.
[11] Chira, A. I., Dumitrescu, A., Moisoiu, C. S., Tanase, C. A., *Human Performance Envelope Model Study Using Pilot's Measured Parameters*, INCAS Bulletin, vol. 12, no. 4, p. 49-61, 2020, DOI: 10.13111/2066-8201.2020.12.4.5.
[12] Edwards, T., Homola, J., Mercer, J., Claudatos, L., *Multifactor interactions and the air traffic controller: the interaction of situation awareness and workload in association with automation*, Cognition, Technology & Work, vol. 19, pp. 687-698, 2017.
[13] Kirwan, B., Wies, M., Charles, R., Dormoy, C. A., Letouze, T., Lemkadden, A., Maille, N., Nixon, J., Ruscio, D., Schmidt-Moll, C., *Charting the edges of human performance,* In MATEC Web of Conferences, vol. 304, EDP Sciences, p. 06007, eISSN: 2261-236X. 2019.
[14] INCAS *Press release* – chrome extension://efaidnbmnnnibpcajpcglclefindmkaj/https://www.incas.ro/wp-content/uploads/2024/04/INCAS-AXIS-KingAir-2024.pdf
[15]https://www.axis-simulation.com/company/
[16] Rusu, V., Calefariu, G., *Measurement of pilots' fatigue, attention and vigilance using EEG, ECG and EYE tracking in the simulated environment*, INCAS Bulletin, vol.17, issue 4, pp. 193-209, 2025.
[17] Hart, S. G., Staveland, L. E., *Development of NASA-TLX (Task Load Index): Results of empirical and theoretical research,* Advances in psychology, vol. 52, pp. 139-183, 1988, North-Holland.
[18] https://www.tobii.com
[19]https://www.biopac.com/product/mp160-system-with-acqknowledge
[20] Nyström, M., Andersson, R., Niehorster, D. C., R. Hessels, S., Hooge, I. T., *What is a blink? Classifying and characterizing blinks in eye openness signals*, Behavior Research Methods, vol. 56, no. 4, pp. 3280-3299, 2024.

Aplicarea modelului matematic asupra măsurătorilor fiziologice ale pilotului

Rezumat: Industria aerospațială se află într-o evoluție continuă; cu toate acestea, conform statisticilor, în anul 2024 numărul accidentelor a crescut față de ultimul deceniu. Printre strategiile promovate de ICAO pentru consolidarea siguranței aeronautice este optimizarea condițiilor de muncă ale personalului. Un exemplu este proiectul Future Sky Safety, care propune o paradigmă ergonomică prin introducerea conceptului Anvelopa Performanței Umane. În lucrările anterioare a fost propusă o definiție a conceptului, a fost delimitat stadiul actual, s-a dezvoltat un model matematic pentru investigarea celor nouă factori ergonomici și au fost realizate măsurători fiziologice asupra pilotului, utilizând un simulator de zbor. Obiectivul prezentei lucrări constă în compararea rezultatelor modelului matematic obținute pe baza valorilor selectate din literatura de specialitate cu cele derivate din experimentul desfășurat.

Victoria RUSU, Eng, PhD Student, Transilvania University of Brașov, Faculty of Technological Engineering and Industrial Management, Department of Engineering and Industrial Management, victoria.rusu@unitbv.ro, +40 788 679 577, 13 Pelicanului Street, Brașov, Romania.
Gavrilă CALEFARIU, Professor Eng. PhD, Transilvania University of Brașov, Faculty of Technological Engineering and Industrial Management, Department of Engineering and Industrial Management, g.calefariu@unitbv.ro, +40 788 679 577, 13 Pelicanului Street, Brașov, Romania.